Defence Science Journal, Vol. 63, No. 5, September 2013, pp. 524-530, DOI : 10.14429/dsj.63.3866

Determination and Validation of Parameters for Riedel-Hiermaier-Thoma Concrete Model

Yu-Qing Ding*, Wen-Hui Tang, Ruo-Qi Zhang, and Xian-Wen Ran

National University of Defense Technology, Changsha - 410 073, China

E-mail: yqding_nudt@163.com

ABSTRACT

Numerical modelling of the complex physical processes such as concrete structures subjected to high-impulsive loads relies on suitable material models appropriate for impact and explosion problems. One of the extensive used concrete material models, the RHT model, contains all essential features of concrete materials subjected to high dynamic loading. However, the application of the RHT model requires a set of material properties and model parameters without which reliable results cannot be expected. The present paper provides a detailed valuation of the RHT model and proposes a method of determining the model parameters for C40 concrete. Furthermore, the dynamic compressive and tensile strength function of the model formulation are modified to enhance the performance of the model as implemented in the hydrocode AUTODYN. The performance of the determined parameters of the modified RHT model is demonstrated by comparing to available experimental data, and further verified via simulations of physical experiments of concrete penetration by steel projectiles. The results of numerical analyses are found closely match the penetration depth and the crater size in the front surface of the concrete targets.

Keywords: Concrete, impact, Riedel-Hiermaier-Thoma, RHT model, model calibration

1. INTRODUCTION

Concrete is a kind of widely used structural material in civil and defence construction, and numerical simulations are an important tool in the investigation of the effects of blast and shock on concrete structure. Recent years, research has been conducted to develop efficient and accurate constitutive models[1-4] to improve the fidelity of the numerical simulations. The Riedel-Hiermaier-Thoma (RHT) concrete model, as a coupled damage-viscoplasticity model, developed by Riedel[5] is readily available to all users of the commercial hydrocode AUTODYN[6]. Over the last decade, numerous worldwide applications appeared in publications which deal with dynamic load cases such as projectile penetration, contact detonation, internal and external blast loading. However, the application of the RHT model requires a set of suitable model parameters without which reliable results cannot be expected. Moreover, the standard RHT model implemented in AUTODYN falls short in representing the concrete behaviour under the dynamic compression and tension loading. In present paper, the modifications of using two bilinear dynamic increase factor functions for the compressive and tensile strength were proposed through user codes. Furthermore, a method to determine the parameters for RHT concrete model was proposed, and the determined parameters of C40 concrete were validated by simulations of penetration test.

2. RIEDEL-HIERMAIER-THOMA CONCRETE MODEL

Riedel-Hiermaier-Thoma (RHT) concrete model couple an equation of state (EoS) that account for the porous compaction of concrete with the RHT strength model contains three limit surfaces in stress space which considering pressure, triaxiality and strain rate. The three surfaces respectively describe the elastic limit Y_{el}, failure Y_{fail}, and residual shear strength Y_{res} of the damaged concrete under confined conditions.

2.1 Failure Surface

The failure surface, Y_{fail}, is defined as a function of the strength along the compression meridian $Y_c(p)$ multiplied by the factors $R_3(\theta)$ and F_{rate} which has the form,

$$f(p,\sigma_{eq},\theta,\dot{\varepsilon}) = \sigma_{eq} - Y_{fail}(p,\theta,\dot{\varepsilon}) = \sigma_{eq} - Y_c(p)R_3(\theta)F_{rate}(\dot{\varepsilon}) = 0 \tag{1}$$

$$Y^*_{fail}(p^*,\theta,\dot{\varepsilon}) = Y^*_c(p^*)R_3(\theta)F_{rate}(\dot{\varepsilon}) \tag{2}$$

$$Y^*_c(p^*) = A\times[p^* - f^*_{ttt}F_{rate}(\dot{\varepsilon})]^N \tag{3}$$

where σ_{eq} is the equivalent stress, p is the pressure, θ is the lode angle, $\dot{\varepsilon}$ is the equivalent strain rate, A and N are the two constants. All measures of hydrostatic pressure and deviatoric strength denoted with * are normalized over the uniaxial cylindrical compressive strength f_c. f^*_{ttt} is the normalized

Received 12 February 2013, revised 4 July 2013, online published 25 September 2013

hydrostatic tensile pressure (compressive stresses defined positive).

$R_3(\theta)$ is used to describe reduced strength on shear and tensile meridians. The Lode angle θ describes stress triaxiality and depends on the third invariant J_3 of the stress tensor. The ratio Q_2 of tensile to compressive meridian decreases with increasing pressure. This effect is called 'brittle to ductile transition' and is described by,

$$R_3(\theta)=\frac{2(1-Q_2^2)\cos\theta+(2Q_2-1)\cdot\sqrt{4(1-Q_2^2)\cos^2\theta+5Q_2^2-4Q_2}}{4(1-Q_2^2)\cos^2\theta+(1-2Q_2)^2} \tag{4}$$

$$\cos 3\theta=\frac{3\sqrt{3}J_3}{2J_2^{3/2}},\quad 0\le\theta\le\frac{\pi}{3} \tag{5}$$

$$Q_2=Q_{2,0}+B_Q p^*,\quad 0.5\le Q_2\le 1.0 \tag{6}$$

where $Q_{2,0}$ is tensile to compressive meridian ratio, B_Q is brittle to ductile transition factor.

The term F_{rate} accounts for the rate enhancement of strength for both compression and tension is expressed as a linear function of the strain rate in the logarithmic scale as follow,

$$F_{rate}(\dot\varepsilon)=\frac{f_{cd/td}}{f_{c/t}}=\begin{cases}(\dot\varepsilon/\dot\varepsilon_{c0})^{\alpha} & \text{for compression}\\ (\dot\varepsilon/\dot\varepsilon_{t0})^{\delta} & \text{for tension}\end{cases} \tag{7}$$

where $f_{c/t}$ is the static uniaxial compressive and tensile strength, $f_{cd/td}$ is the dynamic uniaxial compressive and tensile strength, α and δ are the constants. The static strain rate was taken as 3.0×10^{-5} s^{-1} for compression and 3.0×10^{-6} s^{-1} for tension.

2.2 Elastic Limit Surface and Strain Hardening

The initial elastic surface Y_{el} of the virgin material is derived from the failure surface Y_{fail} using the ratio of elastic compressive and tensile stress over the respective ultimate strength F_{el} ($f_{c,el}/f_c$ and $f_{t,el}/f_t$). The elastic surface is consistent with the porous equation of state towards higher pressures involving pore compaction using a parabolic cap function F_{cap}. The upper cap pressure is equal to Hugoniot elastic limit p_{el} of the concrete material, and the lower pressure p_u for cap influence is set to $f_c/3$. The loading surface Y_{load} described by Eqn (10) is scaled between Y_{el} and Y_{fail} controlled by the equivalent plastic strain. The plastic stiffness is specified by the hardening ratio $G_{el}/(G_{el}-G_{pl})$ which is equal to 2.0.

$$Y_{el}^*=Y_{fail}^*\cdot F_{cap}(p)\cdot F_{el} \tag{8}$$

$$F_{cap}(p)=\begin{cases}1 & \text{for } p\le p_u=3/f_c\\ \sqrt{1-[(p-p_u)/(p_0-p_u)]^2} & \text{for } p_u<p\le p_{el}\\ 0 & \text{for } p_{el}\le p\end{cases} \tag{9}$$

$$Y_{load}=Y_{el}+\frac{\varepsilon_{eq}^{pl}}{\varepsilon_{eq}^{pl,load}}(Y_{fail}-Y_{el}),\qquad \varepsilon_{eq}^{pl,load}=\frac{Y_{fail}-Y_{el}}{3G}\left(\frac{G_{el}}{G_{el}-G_{pl}}\right) \tag{10}$$

2.3 Damage Evolution and Residual Surface

When hardening states reach the ultimate strength of the concrete on the failure surface Y_{fail}, damage is accumulated during further inelastic loading controlled by plastic strain according to equation as below,

$$D=\sum\frac{\Delta\varepsilon_p}{\varepsilon_p^f},\qquad \varepsilon_p^f=D_1(p^*-f_{ttt}^*)^{D_2}\ge\varepsilon_{f,min} \tag{11}$$

where $\Delta\varepsilon_p$ is the accumulated plastic strain, $\varepsilon_p^{\,f}$ is the equivalent plastic strain at failure, D_1 and D_2 are the constants. At low pressure, a lower limit of the failure strain is set by introducing $\varepsilon_{f,min}$ to allow for a finite amount of plastic strain to fracture the material in order to suppress fracture from low magnitude tensile waves.

Under a multi-axial state of stress and existing confining pressure, the concrete retains a certain level of shear strength due to friction among crushed particles. The residual strength Y_{res} of the fully damaged concrete is calculated from equation below. The strength Y_{frac} is then interpolated from the strength values for the undamaged material (D=0) at failure surface and the completely damaged material (D=1) described below,

$$\begin{aligned}Y_{res}&=B\cdot(p^*)^M\\ Y_{frac}&=D\cdot Y_{res}+(1-D)\cdot Y_{fail}\end{aligned} \tag{12}$$

2.4 Equation of State

In the RHT model, for pressures between the initial pore crush pressure p_{el} and compacted pressure p_{comp}, the P-α model is employed as follows,

$$\begin{aligned}&p=f(\rho_{matrix},e)\xrightarrow{porous}p=f(\alpha\rho,e)\\ &\alpha=1+(\alpha_0-1)[(p_{comp}-p)/(p_{comp}-p_{el})]^n\end{aligned} \tag{13}$$

where α_0 is the initial porosity, n is the exponent constant.

For the compaction state, EoS has the form described below,

$$p=A_1\mu+A_2\mu^2+A_3\mu^3+(B_0+B_1\mu)\rho_0 e \tag{14}$$

and for the tension state,

$$p=T_1\mu+T_2\mu^2+B_0\rho_0 e \tag{15}$$

where $\mu=\rho/\rho_0-1$, ρ_0 is the initial density, A_1, A_2, A_3, B_0, B_1, T_1 and T_2 are the parameters for polynomial EoS.

3. DETERMINATION OF PARAMETERS

3.1 Strength Parameters

The C40 concrete specimen was made of Portland 42.5 cement, general river sand, limestone aggregate and tap water with a composition of 1 : 1.38 : 2.67 : 0.41 by weight. The initial density of concrete was 2.35 g/cm^3. Cubic specimens was 150 mm in length for uniaxial compression experiment and splitting experiment were prepared and cured for 28 days before the experiment according to Chinese standard GB/T 50081-2002. Both uniaxial compression and splitting experiments were conducted on the instron-1346 material testing system machine. The cubic uniaxial compressive strength f_{cu} was 40 MPa, the splitting tensile strength f_{tp} was 3.1 MPa, and the shear modulus G was 14.5 GPa derived from the elastic modulus E and poisson's ratio v obtained from the uniaxial compression experiment by $G = E/2(1+v)$. Since the size for concrete specimen of Chinese standard is different with other countries (e.g. Germany, cylinder with 150 mm in diameter and 300 mm in height[7]), the uniaxial compressive strength of the same mix proportion concrete will be different by reference to different standards. The conversion coefficient between uniaxial cylindrical and cubic compressive strength is set to 0.8, and the uniaxial tensile strength f_t is approximately equal to f_{tp} by referring Chinese standard GB 50010-2002. Consequently, the uniaxial cylindrical compressive strength f_c was set to 32 MPa, the tensile strength ratio f_t/f_c was equal to 0.1. In addition, the shear strength f_s was defined by strength ratio f_s/f_c which setting to 0.18, together with the parameters $f_{c,el}/f_c$ and $f_{t,el}/f_t$ which setting to 0.53 and 0.7 respectively[8].

In the appendix of GB 50010-2002, several characteristic strengths of concrete under static loading were provided for determine the parameters of certain concrete failure criterion. The characteristic strengths including hydrostatic tensile strength $f_{ttt} = -0.09\ f_c$, uniaxial compressive strength f_c ($p^* = 1/3$, $\tau^*_{oct} = 1$), bi-axial compressive strength f_{cc} ($p^* = 0.853$, $\tau^*_{oct} = 0.603$), triaxial compressive strength f_{txc1} ($p^* = 4.3$, $\tau^*_{oct} = 2.0$) and f_{txc2} ($p^* = 5.5$, $\tau^*_{oct} = 3.3$) were applied to determine the failure strength parameters A, N, $Q_{2,0}$ and B_Q. τ^*_{oct} is the normalized octahedral shear stress.

In the condition of concrete under static compressive loading, the rate enhancement factor F_{rate} is equal to 1.0, θ is equal to 60°, the Eqn (2) becomes as below,

$$Y^*_{fail}(p^*,\theta) = (3/\sqrt{2}) \times \tau^*_{oct} = A \times [p^* - f^*_{ttt}]^N \times R_3(\theta) \qquad (16)$$

The parameters A and N were obtained by three characteristic strengths f_{ttt}, f_c and f_{txc2}, then the equations can be established as,

$$\begin{cases} A \times (1/3 + 0.09)^N = 1 \\ A \times (5.5 + 0.09)^N = (3/\sqrt{2}) \times 3.3 \end{cases} \qquad (17)$$

We get $A = 1.929$, $N = 0.764$. In the condition of concrete under tensile loading, θ is equal to 0°. By plugging A and N into the Eqn (16), the parameters $Q_{2,0}$ and B_Q were obtained by two characteristic strengths f_{cc} and f_{txc1}, then the equations can be established as,

$$\begin{cases} 1.929 \times 0.9433^{0.764} \times (Q_{2,0} + 0.853 B_Q) = (3/\sqrt{2}) \times 0.603 \\ 1.929 \times 4.39^{0.764} \times (Q_{2,0} + 4.3 B_Q) = (3/\sqrt{2}) \times 2.0 \end{cases} \qquad (18)$$

We get $Q_{2,0} = 0.69$, $B_Q = 0.0048$. Fig. 1, illustrates the prediction of the RHT model for the compression (CM) and tension meridians (TM) using the Eqn (16). It is noted that MRHT means using the modified failure strength parameters, while RHT means using the default failure strength parameters in AUTODYN material database[6]. It is obvious that the meridian curves plotted by the modified failure strength parameters are more close to the experimental data[9].

Over the past few decades a great amount of experiments have been carried out on the behaviour of concrete specimens under high rates of uniaxial compressive loading as well as tensile loading. A thorough bibliography of the abundant experimental data can be found[10,11]. A summary of the available experimental data is presented in Figs. 2 (a) and (b) for the cases

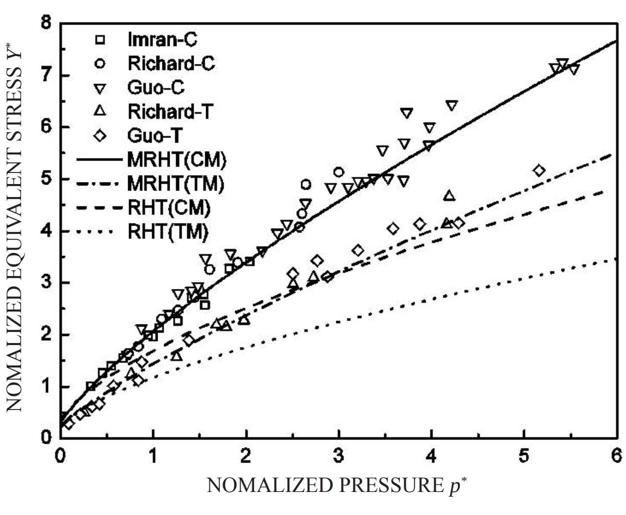

Figure 1. Experimental concrete shear strength response and RHT model prediction.

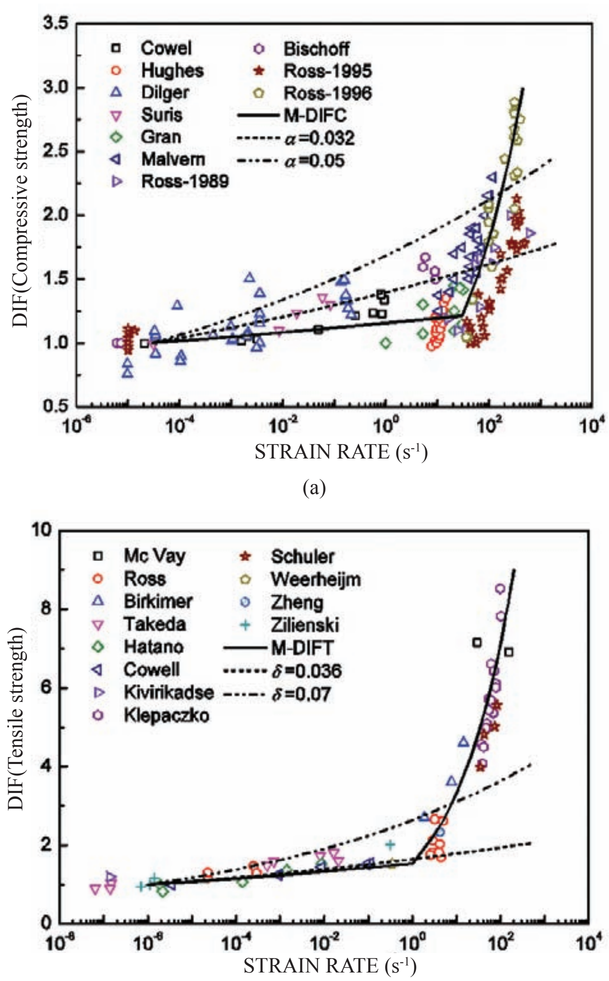

Figure 2. Variation of dynamic increase factor with strain rate for concrete: (a) uniaxial compression, (b) uniaxial compression.

of compressive and tensile loading respectively, expressing the relationship between the DIF (dynamic increase factor, the ratio of the dynamic to static strength) and the strain rate. In the standard RHT model as implemented in AUTODYN, the DIF is determined by the parameter α and δ for compression and tension respectively, see Eqn (7). As seen in Fig. 2, for two values of α and δ, the original DIF cannot be chosen in a way that fits the experimental data. Therefore, a user-defined DIF rectify the dynamic compressive and tensile strength to improve the behaviour of the model referring to Leppanen[12]. The proposed stepwise linear DIF model for compression[7] and tension[12] are described by equations below separately,

$$DIF_c(\dot{\varepsilon}) = \begin{cases} (\dot{\varepsilon}/\dot{\varepsilon}_{c0})^{\alpha_c} & \text{for } \dot{\varepsilon} \le 30s^{-1} \\ \beta_c(\dot{\varepsilon}/\dot{\varepsilon}_{c0})^{1/3} & \text{for } \dot{\varepsilon} > 30s^{-1} \end{cases} \tag{19}$$

$$DIF_t(\dot{\varepsilon}) = \begin{cases} (\dot{\varepsilon}/\dot{\varepsilon}_{t0})^{\delta_t} & \text{for } \dot{\varepsilon} \le 1s^{-1} \\ \beta_t(\dot{\varepsilon}/\dot{\varepsilon}_{t0})^{1/3} & \text{for } \dot{\varepsilon} > 1s^{-1} \end{cases} \tag{20}$$

where subscript c and t represent compression and tension respectively, the static strain rate is taken as 3.0×10^{-5} s^{-1} for compression and 1.0×10^{-6} s^{-1} for tension. α_c and β_c were equal to 0.014 and 0.012 respectively[7]. $\delta_t = 0.031$ and $\beta_t = 0.015$ were obtained based on the experimental data. It is obvious that the implemented DIF fit the experimental data well.

Because of the residual surface can so far not be measured[8], the residual strength parameters B and M cannot be determined by experimental data. However, the parametric studies, conducted by leppanen[12], indicate that the simulation results were reasonable and fit the experiment results well by setting B and M equal to 1.50 and 0.70, respectively.

3.2 Damage Parameters

The uniaxial cyclic loading and unloading experiments were performed on cylindrical concrete specimens with 50 mm in diameter and 100 mm in height, and the repeated experiments were conducted to ensure the reliability of experimental results. The representative stress-strain curve was illustrated in Fig. 3. An assumed failure surface was defined from the test results, indicating a total loss in strength at an axial strain of ε_x. During the loading process, the elastic strain ε_{xe} and the volumetric strain μ can be neglected due to the early curvature of modulus and the low pressures (0-f_c/3) that occur respectively, as shown in Fig.3. By assuming $\varepsilon_{xe} = \mu = 0$, the equivalent plastic strain at failure ε_p^f was equal to ε_x. Initiating the damage curve at $f_{ttt}^* = -0.09$ and satisfying ε_p^f at $\bar{p}^* = 1/6$ (average from $p^* = 0$ to $p^* = 1/3$), the constant D_1 was obtained by the Eqn (21),

$$D_1 = \frac{\varepsilon_p^f}{(\bar{p}^* - f_{ttt}^*)^{D_2}} \tag{21}$$

where ε_p^f was equal to 0.013 obtained from the experiment, and $\varepsilon_{f,min}$, D_2 was set to default value[6].

3.3 Equation of State Parameters

In order to derive the EoS parameters of the large scale heterogeneous mixture material such as concrete, it is necessary to decompose the concrete into smaller scale homogeneous components mortar and aggregate, to measure the hugoniot properties separately. A hugoniot mixing rule[13] based on the mass-weighted contribution of each component to density ρ, bulk sound speed c_B, slope s of the shock particle velocity and the Grüneisen parameter γ were applied as below,

$$\rho_0 = \sum m_i \rho_{0i}, c_B = \sum m_i c_{Bi}, s = \sum m_i s_i, \gamma = \sum m_i \gamma_i \tag{22}$$

The mortar specimens were made of the same proportion as concrete specimens just removing the aggregates, and cured for 28 days prior to the experiments. The density of mortar specimen was measured to be 2.10 g/cm^3. Plate impact experiments were performed using one stage light gas gun facility with a bore diameter of 57 mm and an impact velocity ranging from 190 m/s to 500 m/s, to obtain stress levels ranging from 0.5 GPa to 2 GPa. Fig. 4 shows the plate configuration just before impact. The geometry of target and projectile, restricted by the bore diameter of 57 mm, was investigated by pre-test numerical analysis to prevent release wave effects during experimental data acquisition. The projectile consists of a 7 mm thick flyer mounted on the front of a sabot which both made of 2024 aluminium alloy. Sequential pin-shorting method was used to measure impact velocities and tilt was fixed to be less than 1 mrad by means of an adjustable specimen mount. The target consists of three 4.8 mm thick mortar specimens in the

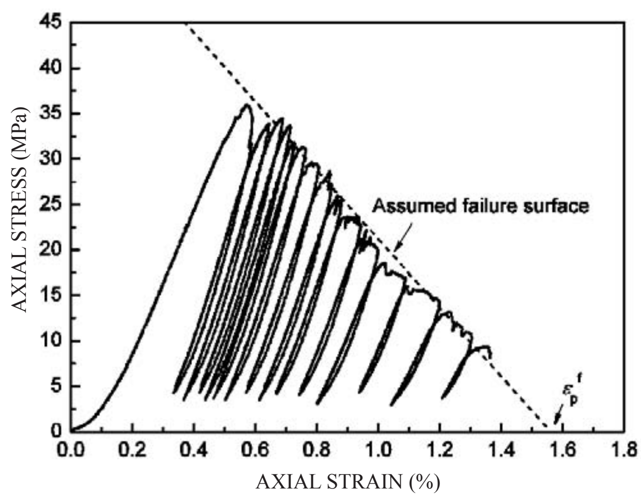

Figure 3. The stress-strain curve from uniaxial cyclic loading and unloading experiment.

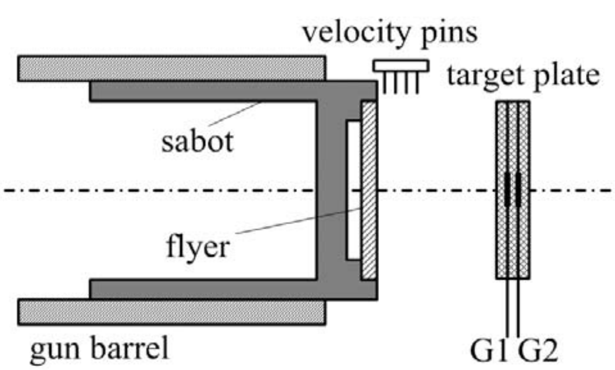

Figure 4. Configuration of planar impact experiment.

impact direction, and the target device was aligned to accuracy below 1 mrad, longitudinal stress measurements were taken by embedding piezoresistive manganin gauges between ties of the target material using a low viscosity epoxy adhesive. Fig. 5(a) illustrates some representative stress wave profiles as obtained from the gauges. The shock velocity D in mortar specimen can be obtained from the thickness of the middle specimen L and the time duration Δt measured by the two gauges. The detail experimental results were listed in Table 1. By using the impedance matching relations at boundaries between different materials[13], the hugoniot of mortar obtained is shown below in Fig. 5(b). The relationship between shock wave velocity D and the particle's velocity after shock wave u is $D = 3.24 + 1.15\ u$ (km/s), that is, $c_{B1} = 3.24$ km/s, $s_1 = 1.15$. The hugoniot parameters of limestone were $c_{B2} = 3.40$ km/s, $s_2 = 1.54$ according to Ahrens[14]. In addition, the Dugdale and Macdonald's approximation[13] for the Grüneisen coefficient γ is applied, $\gamma = 2s–1$. By using the Eqn (22), based on the composition of concrete, the hugoniot parameters of concrete were obtained: $c_B = 3.32$ km/s, $s = 1.34$, $\gamma = 1.68$. Furthermore, the parameters of the polynomial equation of state can be obtained by the equations as follows,

$$\begin{aligned} A_1 &= T_1 = \rho_{s0} c_B^2 \\ A_2 &= \rho_{s0} c_B^2 [1 + s(s-1)] \\ A_3 &= \rho_{s0} c_B^2 [2(s-1) + 3(s-1)^2] \\ B_0 &= B_1 = \gamma \end{aligned} \tag{23}$$

where ρ_{s0} is the compacted density of concrete which setting to 2.75 g/cm^3 by reference to Riedel[8]. We get $A_1 = T_1 = 30.3$ GPa, $A_2 = 44.1$ GPa, $A_3 = 31.1$ GPa, $B_0 = B_1 = 1.68$. The parameter T_2 was set to zero[6].

The porous soundspeed c_p was 2950 m/s measured by ZBL-U520 non-mental ultrasonic testing device. In addition, p_{el}, p_{comp} and n were set to $2/3f_c$, 6 GPa, and 3 respectively[8]. These values are assumed to be identical for all practicable concrete.

4. NUMERICAL SIMULATION OF PENETRATION INTO CONCRETE

For testing the predictive quality of the model parameters in the simulation of impact processes, the results of numerical simulation were compared to the penetration tests reported by Hansson[15]. In the experiments the steel projectiles with an ogive nose of caliber-radius-head (CRH) 3.0, a length of 225 mm and a diameter of 75 mm were fired with zero attack angle into massive cylindrical concrete targets with a diameter of 1.6 m and a length of 2.0 m. The total mass of the projectile was 6.28 kg. The steel material had the following properties: bulk modulus 159 GPa, shear modulus 81.8 GPa, and yield stress 792 MPa. The compressive strength of 150 mm cubic concrete was about 40 MPa. The impact velocity and penetration depth were measured to be 485 m/s and 655 mm - 660 mm from two

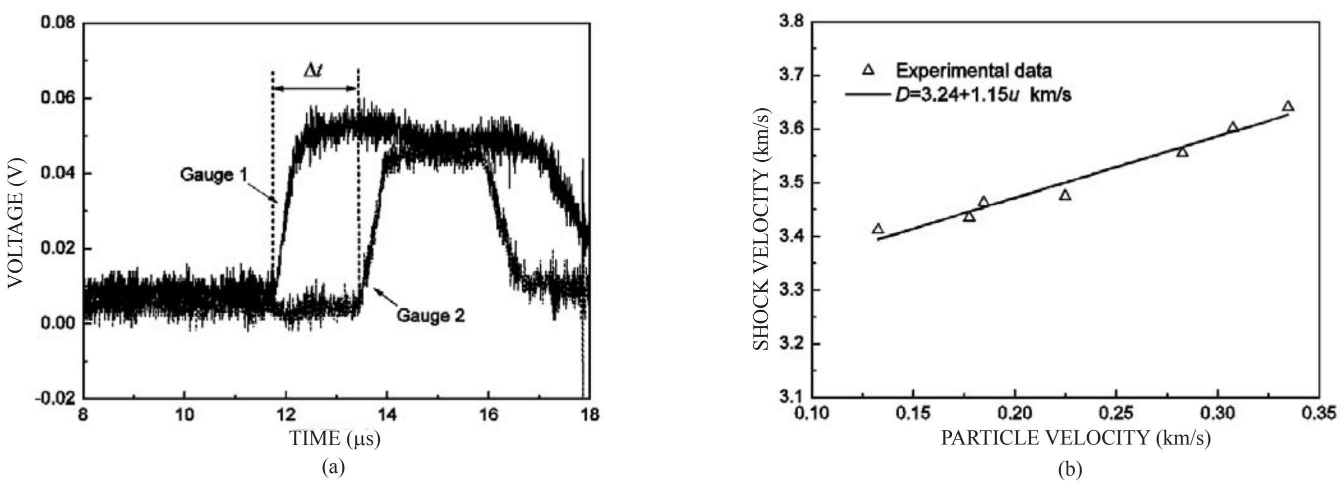

Figure 5. The results of plate impact experiment: (a) The output of the gauges from experiment with impact velocity of 0.332 km/s, (b) Hugoniot data for mortar specimen: shock velocity D *vs* particle velocity u.

Table 1. Experimental parameters and hugoniot data for mortar

Shot No.	Specimen thickness (mm)	Impact velocity (km/s)	Time duration (μs)	Shock velocity (km/s)	Particle velocity (km/s)	Pressure (GPa)
1#	4.77	0.500	1.31	3.641	0.335	2.558
2#	4.79	0.458	1.33	3.602	0.307	2.325
3#	4.80	0.420	1.35	3.556	0.283	2.110
4#	4.83	0.332	1.39	3.475	0.225	1.640
5#	4.71	0.273	1.36	3.463	0.185	1.343
6#	4.74	0.262	1.38	3.435	0.177	1.280
7#	4.88	0.196	1.43	3.413	0.133	0.950

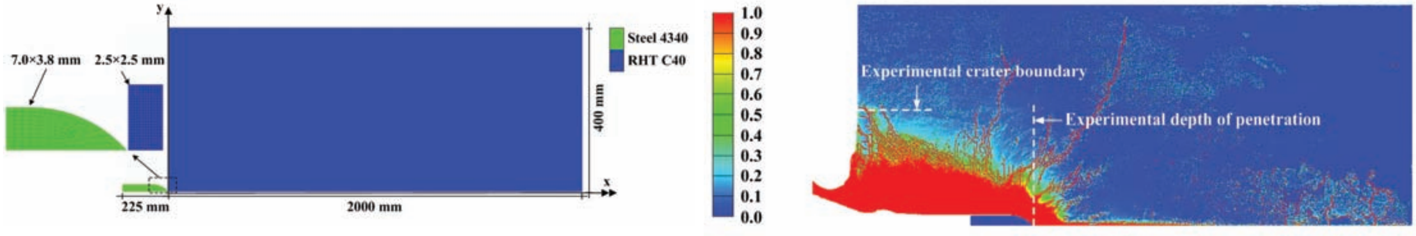

(a) (b)

Figure 6. Numerical simulation of penetration into concrete target: (a) model set-up and discretization, (b) numerical and experimental results.

Table 2. The parameters for C40 concrete of RHT model

f_c (MPa)	G (GPa)	f_s/f_c	f_t/f_c	$f_{c,el}/f_c$	$f_{t,el}/f_t$	A	N
32	14.5	0.18	0.10	0.53	0.7	1.929	0.764
$Q_{2,0}$	B_Q	α_c	β_c	δ_t	β_t	B	M
0.69	0.0048	0.014	0.012	0.031	0.015	1.50	0.70
D_1	D_2	$\varepsilon_{f,min}$	ρ_0 (g/cm^3)	c_p (m/s)	ρ_{s0} (g/cm^3)	p_{el} (MPa)	P_{comp} (GPa)
0.051	1.0	0.01	2.35	2950	2.75	21.3	6.0
n	A_1 (GPa)	A_2 (GPa)	A_3 (GPa)	B_0	B_1	T_1 (GPa)	T_2 (GPa)
3	30.3	44.1	31.1	1.68	1.68	30.3	0

shots, respectively. The dimension of the crater produced was also measured and the diameter was about 800 mm. A numerical model of the experiments was set up which schematically illustrated in Fig. 6(a). The concrete targets were discretized in a 2.5 × 2.5 mm Lagrangian mesh applying the RHT model parameters determined in the previous sections exhibited in Table 2. The projectile was also modelled in a Lagrangian mesh with a mesh size of between 7.0 × 3.75 mm in the rear part and 8.4 × 3.75 mm in the projectile nose applying the material model Steel 4340 from the AUTODYN material library. The experiments were simulated and the penetration depths were determined after the projectile had stopped. The numerical and experimental results generally show a good agreement as shown in Fig. 6(b).

5. CONCLUSIONS

The Riedel-Hiermaier-Thoma (RHT) material model takes account of many important features of concrete under high-impulsive loading. Concrete has a great variety of strength grades, but only 35 MPa and 135 MPa concrete parameters are provided in AUTODYN material database. Moreover, the standard RHT model implemented in AUTODYN falls short in representing the concrete behaviour under the dynamic compression and tension loading. Therefore, the modifications of using two bi-linear dynamic increase factor functions for the compressive and tensile strength are proposed through user codes. With the modifications, the RHT model is found to behave more realistically in modelling the concrete behaviour in compression as well as in tension. Furthermore, the present paper proposes a method to determine the RHT model parameters, and the RHT model parameters for C40 concrete were obtained. Numerical simulation of penetration of concrete targets by steel projectile is conducted to further evaluation of the performance of the modified RHT model using the determined parameters in real applications. The numerical simulation results were in appreciable good agreement with experimental results.

REFERENCES

1. Brannon, R.M.; Leelavanichkul, S. Survey of Four Damage Models for Concrete. Sandia Laboratories, Albuquerque. Sandia Report No. SAND 2009-5544. August 2009.
2. Babu, R.R.; Benipal, G.S. & Singh, A.K. Constitutive model for bimodular elastic damage of concrete. *Latin American J. Solids and Structures*, 2010, **7**(2), 143-66.
3. Lu, G.; Li, X. & Wang, K. A numerical study on the damage of projectile impact on concrete targets. *Computers & Concrete*, 2012, **9**(1), 21-33.
4. Mu, Z.C.; Dancygier, A.N.; Zhang, W. & Yankelevsky, D.Z. Revisiting the dynamic compressive behavior of concrete-like materials. *Int. J. Impact. Engg.*, 2012, **49**, 91-102.
5. Riedel, W. Beton unter dynamischen lasten meso-und makromechanische modelle und ihre parameter. Ernst-Mach-Institute, Freiburg, Germany, 2000. PhD Thesis. (German)
6. ANSYS Autodyn v13.0 user manual. ANSYS Inc. Canonsburg, USA, 2010.
7. FIB. Model code 2010 (first complete draft), Lausanne, Switzerland, FIB Bulletin 55, vol. 1, 2010.
8. Riedel, W.; Kawai, N. & Kondo, K. Numerical assessment for impact strength measurements in concrete materials.

Int. J. Impact. Engg., 2009, **36**(2), 283-93.
9. Guo, Z.H.; Wang, C.Z. Investigation of strength and failure criterion of concrete under multi-axial stresses. *China Civil Engg. J.*, 1991, **24**(3), 1-14. (Chinese).
10. Bischoff, P.H.; Perry, S.H. Compressive behaviour of concrete at high strain rates. *Materials and Structures*, 1991, **24**(6), 425-50.
11. Cotsovos, D.M.; Pavlovic, M.N. Numerical investigation of concrete subjected to high rates of uniaxial tensile loading. *Int. J. Impact. Engg.*, 2008, **35**(5), 319-35.
12. Leppaen, J. Concrete subjected to projectile and fragment impacts, Modelling of crack softening and strain rate dependency in tension. *Int. J. Impact. Engg.*, 2006, **32** (11), 1828-41.
13. Tang, W.H.; Zhang, R.Q. Introduction to Theory and Computation of Equation of State. Higher Education Press, Beijing, 2008. 306p. (Chinese).
14. Ahrens, T.J.; Johnson, M.L. Shock wave data for rocks. Rock Physics and Phase Relations, A Handbook of Physical Constants, *edited by* Ahrens, T.J. American Geophysical Union, Washington DC, USA, 1995, pp. 35-44.
15. Hansson, H. Numerical simulation of concrete penetration. FOA-Swedesh Defence Research Agency, Technical Report No. FOA-98-00816-311-SE. 1998.

CONTRIBUTORS

Mr Yuqing Ding obtained his Master's degree from National University of Defense Technology, China, in 2009. He is pursuing PhD at NUDT. His research areas are engineering mechanics and the vulnerability of targets.

Dr Wenhui Tang obtained his PhD from National University of Defense Technology, China, in 1995. At present, he is Professor at Institute of Engineering Physics, NUDT. His research interests are explosion mechanics, the vulnerability of targets, and shock wave physics.

Mr Ruoqi Zhang is Professor at Institute of Engineering Physics, NUDT. His research interests are in shock wave physics, explosion mechanics and explosion protection.

Dr Xianwen Ran obtained his PhD from National University of Defense Technology, China, in 2006. He is working as a Lecturer at Institute of Engineering Physics, NUDT. His research interests are explosion mechanics, the vulnerability of targets, and shock induced phase transition.